

A New Method for Dynamic Impedance of Foundation on Saturated Poroelastic Soil

S.L. Chen, C. Zhen

Department of Civil Engineering, Nanjing University of Aeronautics and Astronautics, Nanjing 210016, China



SUMMARY:

Based on the method of lumped-mass explicit finite element and local transmitting artificial boundary, a time domain method is presented for the computation of dynamic stiffness of rigid foundations resting on or embedded in saturated poroelastic soil. The two-phase behavior of porous medium is represented according to Biot's theory. The technique is applied to the computation of dynamic stiffness of rigid plate on a saturated poroelastic half-space. Compliance component are computed and compared with existing results. The effects of permeability, the embedded depth on the dynamic stiffness are examined. The technique presented in this paper is able to represent more general properties and geometries of soil and foundation than do the existing approaches.

Keywords: Saturated poroelastic medium Transmitting artificial boundary Dynamic stiffness of foundation

1. INTRODUCTION

The analysis of the dynamic force-displacement relationship of a rigid massless foundation resting on a uniform half-space or on a layered stratum plays an important role in the seismic response analysis of structures and in the study of machine vibrations. Traditionally, evaluating the foundation impedance functions has been based on the assumption that the subgrade is either an elastic or a viscoelastic solid. Often, however, a soil subgrade may be more properly regarded as a liquid-filled poroelastic solid.

The theory of propagation of elastic waves in a fluid-saturated porous solid was presented by Biot(1956). Based on the Biot's theory for dynamic behavior of poroelastic media, Halpern and Christiano(1986) computed compliance coefficients of rigid plates on the surface of a three-dimensional saturated poroelastic half-space. They integrated Green functions over the elements in which the foundation is subdivided and presented vertical and rocking compliance for a square rigid plate bearing on a water saturated poroelastic half-space for water saturated coarse grained sands. Kassir and Xu(1988) carried out a similar study for a strip footing on a two-phase poroelastic half-space. Bougacha et al.(1993) obtained dynamic stiffness of strip and circular foundation on two-phase poroelastic stratum by a finite-element approach based on the use of spatially semidiscrete modes of vibration. It is limited to footings on horizontally layered soils that extend to infinity and are based on a rigid bedrock. Using a Laplace domain boundary element formulation, Chen and Dargush(1995) and Chopra and Dargush(1995) have also obtained some impedance functions for rigid foundations on poroelastic soils. Based on the boundary element formulation, Japon et al. (1997) obtained dynamic stiffness coefficients of strip foundations on two-phase poroelastic soils. Philippacopoulos(1989) present dynamic stiffness for vertical motion of a rigid disk foundation on a layered poroelastic half-space saturated up to certain depth below the disk. Rajapakse and Senjuntichai (1995) present a soil-structure interaction model for rigid strip foundation on a layered half-space.

The aim of this study is to present a new numerical approach that can be used to obtain dynamic stiffness coefficients and the seismic response of three-dimensional foundations, resting on or embedded in saturated poroelastic soils. Although the results presented are only for half-space, the technique is very versatile and the analysis of more complicated underground geometries only require a different element mesh.

2. MATHEMATICAL FORMULATION

According to the definition of foundation impedance, if the foundation is given a pulse displacement on one freedom with other freedoms fixed, the problem of impedance is how to calculate the forces exerted on the foundation. We consider the response of a fluid-saturated poroelastic half-space to pulse displacement excitation of a rigid, impervious massless plate resting on the surface or embedded in the soil, as shown in Fig.2.1. This is a relaxed mixed-boundary-value problem in which displacement constraints are imposed by the rigid plate while the region outside the plate is traction-free. The forces exerted on the foundation by the soil are of interest. Once they are computed, the dynamic impedance of the foundation can be evaluated.

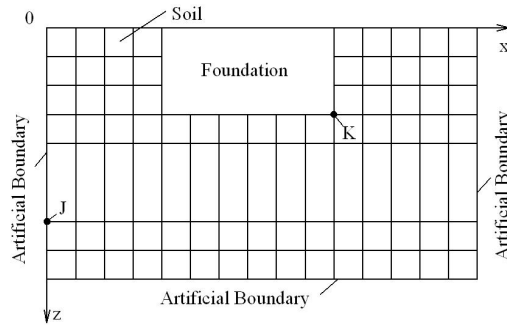


Figure 2.1 Calculation model

The governing equations of motion derived by Biot(1956) may be expressed as:

$$N\nabla^2\mathbf{u} + \nabla[(A+N)e + Q\varepsilon] = \frac{\partial^2}{\partial t^2}(\rho_{11}\mathbf{u} + \rho_{12}\mathbf{U}) + b\frac{\partial}{\partial t}(\mathbf{u} - \mathbf{U}) \quad (2.1)$$

$$\nabla[Qe + R\varepsilon] = \frac{\partial^2}{\partial t^2}(\rho_{12}\mathbf{u} + \rho_{22}\mathbf{U}) - b\frac{\partial}{\partial t}(\mathbf{u} - \mathbf{U}) \quad (2.2)$$

where, \mathbf{u} and \mathbf{U} represent, respectively, displacements of the solid and fluid phases as vector functions of x, y, z ; e and ε are volumetric strains of solid and fluid phases, respectively; A, N, Q and R are material constants; $A = \lambda + M(\alpha - n)^2$, $N = \mu$, $Q = n(\alpha - n)M$, $R = n^2M$; n is

porosity, λ and μ are Lamé constants for the solid skeleton; $M = \frac{(E_u)^2 E_w}{n(E_u)^2 + (1-n)E_u E_w - E_b E_w}$,

$\alpha = 1 - E_b/E_u$, E_b and E_u represent, respectively, compressive module for undrained and drained condition; E_w is compressive module of porous fluid; $\rho_{11} = \rho_1 + \rho_\alpha$, $\rho_1 = (1-n)\rho_s$, $\rho_{12} = -\rho_\alpha$, $\rho_2 = n\rho_w$, $\rho_{22} = \rho_2 + \rho_\alpha$, ρ_s and ρ_w describe, respectively, the densities of the solid and fluid phases, while ρ_α describes inertial coupling between the two phase; and $b = \eta n^2/k$, η is viscous coefficients of fluid and k is permeability.

The soil is modeled using eight-node hexahedral elements. Each node has three translational degrees of freedom along x, y and z coordinates. Having discretized the region bounded by the artificial

boundary using FEM, the discrete nodes of soil subsystem are divided into three groups: the boundary nodes which are on the artificial boundary, the nodes which are connected with the rigid foundation, and the interior nodes which include all the others. The motions of these nodes will be discussed in this section.

2.1. The motions of soil node connected with foundation

The motion of the rigid foundation is described by six degrees of freedom: three translations and three rotations.

$$\mathbf{U}_F = \{u_{fx}, u_{fy}, u_{fz}, \theta_{fx}, \theta_{fy}, \theta_{fz}\}^T \quad (2.3)$$

On the assumption that the connection between soil and foundation is bonded perfectly, the motions of node connecting soil with foundation can be decided by foundation motion

$$\mathbf{u}_k = \mathbf{A}\mathbf{U}_F \quad (2.4)$$

where, \mathbf{u}_k is displacement vector of soil node k connected with foundation; \mathbf{A} is transformation matrix, ΔX_k , ΔY_k and ΔZ_k are the coordinates of node k with respect to center of mass of the foundation.

$$\mathbf{A} = \begin{bmatrix} 1 & 0 & 0 & 0 & \Delta Z_k & -\Delta Y_k \\ 0 & 1 & 0 & -\Delta Z_k & 0 & \Delta X_k \\ 0 & 0 & 1 & \Delta Y_k & -\Delta X_k & 0 \end{bmatrix} \quad (2.5)$$

2.2. The motions of interior node

The governing equations of the interior nodes may be set up using the standard finite element technique. What should be noted is that the lumped-mass formulation is suggested for the spatial discretization in this study. This is because the lumped-mass formulation combined with explicit time integration scheme is efficient for large-scale computations. The governing equations of the interior nodes are written in the following form (Chen and Liao,2007).

For solid phase:

$$\ddot{\mathbf{u}}_i \mathbf{M}_{si} + \sum_{e=1}^N \sum_{j=1}^J (\mathbf{C}_{ssk(i)j}^e \dot{\mathbf{u}}_j^e - \mathbf{C}_{swk(i)j}^e \dot{\mathbf{U}}_j^e + \mathbf{K}_{ssk(i)j}^e \mathbf{u}_j^e + \mathbf{K}_{swk(i)j}^e \mathbf{U}_j^e) = \sum_{e=1}^N \mathbf{F}_{si}^e \quad (2.6)$$

for fluid phase:

$$\ddot{\mathbf{U}}_i \mathbf{M}_{wi} + \sum_{e=1}^N \sum_{j=1}^J (-\mathbf{C}_{wsk(i)j}^e \dot{\mathbf{u}}_j^e + \mathbf{C}_{wwk(i)j}^e \dot{\mathbf{U}}_j^e + \mathbf{K}_{wsk(i)j}^e \mathbf{u}_j^e + \mathbf{K}_{wwk(i)j}^e \mathbf{U}_j^e) = \sum_{e=1}^N \mathbf{F}_{wi}^e \quad (2.7)$$

where, $\ddot{\mathbf{u}}_i$ and $\ddot{\mathbf{U}}_i$ are, respectively, displacement vectors of solid phase and fluid phase for node i ; \mathbf{u}_j^e and $\dot{\mathbf{u}}_j^e$ represent, respectively, displacement and velocity vectors of solid phase for node j in element e ; \mathbf{U}_j^e and $\dot{\mathbf{U}}_j^e$ represent, respectively, displacement and velocity vectors of fluid phase for node j in element e ; \mathbf{M}_{si} and \mathbf{M}_{wi} are lumped mass matrix of solid phase and fluid phase for node i , respectively; $\mathbf{C}_{ssk(i)j}^e$, $\mathbf{C}_{swk(i)j}^e$, $\mathbf{C}_{wsk(i)j}^e$ and $\mathbf{C}_{wwk(i)j}^e$ are part of element damping matrix. $\mathbf{K}_{ssk(i)j}^e$, $\mathbf{K}_{swk(i)j}^e$, $\mathbf{K}_{wsk(i)j}^e$ and $\mathbf{K}_{wwk(i)j}^e$ are part of element stiffness matrix; \mathbf{F}_{si}^e and \mathbf{F}_{wi}^e denote, respectively, the external nodal force vectors of solid phase and fluid phase for node i . N is

number of element which include node i . J is number of node for element e .

After implementation of explicit time integration which results from the combination of center difference scheme and Newmark scheme, Eqn.2.6 and Eqn.2.7 can be expressed as (Chen and Liao,2007)

For displacement:

$$\begin{aligned} \mathbf{u}_i^{p+1} = & -\frac{\Delta t^2}{2} \mathbf{M}_{si}^{-1} \sum_{e=1}^N \sum_{j=1}^J (\mathbf{C}_{ssk(i)j}^e \dot{\mathbf{u}}_j^{ep} - \mathbf{C}_{swk(i)j}^e \dot{\mathbf{U}}_j^{ep} + \mathbf{K}_{ssk(i)j}^e \mathbf{u}_j^{ep} \\ & + \mathbf{K}_{swk(i)j}^e \mathbf{U}_j^{ep}) + \mathbf{u}_i^p + \Delta t \dot{\mathbf{u}}_i^p + \frac{\Delta t^2}{2} \mathbf{M}_{si}^{-1} \sum_{e=1}^N \mathbf{F}_{si}^{ep} \end{aligned} \quad (2.8)$$

$$\begin{aligned} \mathbf{U}_i^{p+1} = & -\frac{\Delta t^2}{2} \mathbf{M}_{wi}^{-1} \sum_{e=1}^N \sum_{j=1}^J (-\mathbf{C}_{wsk(i)j}^e \dot{\mathbf{u}}_j^{ep} + \mathbf{C}_{wwk(i)j}^e \dot{\mathbf{U}}_j^{ep} + \mathbf{K}_{wsk(i)j}^e \mathbf{u}_j^{ep} \\ & + \mathbf{K}_{wwk(i)j}^e \mathbf{U}_j^{ep}) + \mathbf{U}_i^p + \Delta t \dot{\mathbf{U}}_i^p + \frac{\Delta t^2}{2} \mathbf{M}_{wi}^{-1} \sum_{e=1}^N \mathbf{F}_{wi}^{ep} \end{aligned} \quad (2.9)$$

for velocity:

$$\begin{aligned} \dot{\mathbf{u}}_i^{p+1} = & \dot{\mathbf{u}}_i^p - \mathbf{M}_{si}^{-1} \sum_{e=1}^N \sum_{j=1}^J (\mathbf{C}_{ssk(i)j}^e (\mathbf{u}_j^{e(p+1)} - \mathbf{u}_j^{ep}) - \mathbf{C}_{swk(i)j}^e (\mathbf{U}_j^{e(p+1)} - \mathbf{U}_j^{ep})) \\ & + \frac{\Delta t}{2} \mathbf{M}_{si}^{-1} \sum_{e=1}^N \left\{ (\mathbf{F}_{si}^{e(p+1)} + \mathbf{F}_{si}^{ep}) - \sum_{j=1}^J (\mathbf{K}_{ssk(i)j}^e (\mathbf{u}_j^{e(p+1)} + \mathbf{u}_j^{ep}) \right. \\ & \left. + \mathbf{K}_{swk(i)j}^e (\mathbf{U}_j^{e(p+1)} + \mathbf{U}_j^{ep})) \right\} \end{aligned} \quad (2.10)$$

$$\begin{aligned} \dot{\mathbf{U}}_i^{p+1} = & \dot{\mathbf{U}}_i^p - \mathbf{M}_{wi}^{-1} \sum_{e=1}^N \sum_{j=1}^J (-\mathbf{C}_{wsk(i)j}^e (\mathbf{u}_j^{e(p+1)} - \mathbf{u}_j^{ep}) + \mathbf{C}_{wwk(i)j}^e (\mathbf{U}_j^{e(p+1)} - \mathbf{U}_j^{ep})) \\ & + \frac{\Delta t}{2} \mathbf{M}_{wi}^{-1} \sum_{e=1}^N \left\{ (\mathbf{F}_{wi}^{e(p+1)} + \mathbf{F}_{wi}^{ep}) - \sum_{j=1}^J (\mathbf{K}_{wsk(i)j}^e (\mathbf{u}_j^{e(p+1)} + \mathbf{u}_j^{ep}) \right. \\ & \left. + \mathbf{K}_{wwk(i)j}^e (\mathbf{U}_j^{e(p+1)} + \mathbf{U}_j^{ep})) \right\} \end{aligned} \quad (2.11)$$

where, Δt is the time step, \mathbf{u}_i^p and \mathbf{U}_i^p are the displacement vectors of node i at time $p\Delta t$ for solid and fluid phase respectively, \mathbf{u}_j^{ep} and \mathbf{U}_j^{ep} are displacement vectors of node j for element e at time $p\Delta t$.

2.3. Artificial boundary condition

Considering the attenuation character of wave motion in two-phase media, we have generalized the MTF(Multi-Transmitting Formula)(Liao and Wong,1984) into the case of two-phase media. The detailed derivation can refer to (Chen and Liao, 2003), only the final formulas are given below:

$$\Phi \mathbf{u}_0^{p+1} = 0 \quad \Phi \mathbf{U}_0^{p+1} = 0 \quad (2.12)$$

$$\Phi = \prod_{m=1}^L \left(B_0^0 - t_{1,1}^m B_0^1 - t_{1,2}^m \delta_m B_1^1 - t_{1,3}^m (\delta_m)^2 B_2^1 \right) \quad (2.13)$$

$$\begin{aligned} \delta_m &= \exp(-\beta_{am}\Delta x), \quad t_{1,1}^m = (2 - S_m)(1 - S_m)/2 \\ t_{1,2}^m &= S_m(2 - S_m), \quad t_{1,3}^m = S_m(S_m - 1)/2, \quad S_m = c_{am}\Delta t / \Delta x \end{aligned} \quad (2.14)$$

where, Δx is the spatial step, \mathbf{u}_0^{p+1} and \mathbf{U}_0^{p+1} are the displacement vectors of artificial boundary point at time $(p+1)\Delta t$ for solid and fluid phase respectively, L is the order of the generalized MTF, c_{am} and β_{am} are the m th artificial wave speed and artificial attenuation coefficient respectively, B_j^q is a backward operator with

$$B_j^q \mathbf{u}_n^p = \mathbf{u}_{n+j}^{p-q} \quad (2.15)$$

where, \mathbf{u}_n^p and \mathbf{U}_n^p are the displacement vectors at $x = -n\Delta x$ on the x -axis, which coincides with the outward normal to the artificial boundary at the boundary point 0, with the boundary point 0 as its origin. The Eqn.2.12 is the generalized MTF for attenuation waves in two-phase media, which can be reduced to the MTF when the attenuation coefficients are zero. Moreover, the generalized MTF is independent of any specific model and local in time and space.

2.4. Procedure of calculating foundation impedance

Assuming that the responses of the soil-foundation system are known before time $p\Delta t$, the responses at time $(p+1)\Delta t$ can be calculated as follows:

- (1) Given the displacement of rigid foundation, $u_F((p+1)\Delta t)$, the displacements of soil node connecting with foundation can be obtained by Eqn.2.4 and Eqn.2.5.
- (2) The displacements of interior soil node at time $(p+1)\Delta t$ can be calculated using Eqn.2.8 and Eqn.2.9.
- (3) The displacements of artificial boundary node at time $(p+1)\Delta t$ can be obtained by MTF Eqn.2.12.
- (4) Given the displacements of soil node at time $(p+1)\Delta t$, the force vector $\mathbf{F}((p+1)\Delta t)$ exerted on the foundation by soil at time $(p+1)\Delta t$ can be obtained through FEM procedure.
- (5) Repeating the steps above, the response of the soil-foundation system can be obtained at successive time.

Thus, according to the definition, the foundation impedance can be obtained as

$$\mathbf{K}_s(\omega) = \frac{\mathbf{F}(\omega)}{U_F(\omega)} \quad (2.16)$$

where, $\mathbf{F}(\omega)$ and $U_F(\omega)$ are, respectively, the FFT transformation of $\mathbf{F}(t)$ and $u_F(t)$.

Because of the symmetry of the rectangular foundation, the impedance matrix reduce in this case to the symmetric matrix

$$\mathbf{K}_s = \begin{bmatrix} K_{11} & K_{12} & 0 & 0 & 0 & 0 \\ K_{21} & K_{22} & 0 & 0 & 0 & 0 \\ 0 & 0 & K_{33} & K_{34} & 0 & 0 \\ 0 & 0 & K_{43} & K_{44} & 0 & 0 \\ 0 & 0 & 0 & 0 & K_{55} & 0 \\ 0 & 0 & 0 & 0 & 0 & K_{66} \end{bmatrix} \quad (2.17)$$

where, K_{55} is vertical impedance function; K_{11} and K_{33} are horizontal impedance along x axis and y axis, respectively; K_{22} and K_{44} are, respectively, rocking impedance function around y axis and x axis; K_{66} is rotation impedance function; the horizontal-rocking coupling terms $K_{12} = K_{21}$ and $K_{34} = K_{43}$.

For comparison, the dimensionless frequency and dimensionless compliance are defined as follow:

$$A_p = \frac{\omega B}{4\pi c_s} \quad C_{ii} = \frac{G_s B \Delta}{K_{ii}} \quad (i=1,3,5) \quad C_{ii} = \frac{NB^3 \theta}{8K_{ii}} \quad (i=2,4,6) \quad (2.18)$$

where, A_p is dimensionless frequency, and C_{ii} is dimensional compliance; B is width of the foundation; $c_s = \sqrt{(G_s/\rho_s)}$ is velocity of shear wave; Δ and θ represent, respectively, the unit displacement and unit rotation.

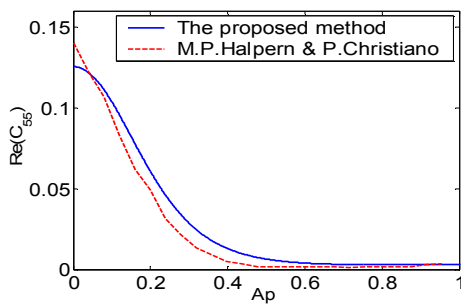
3. NUMERICAL EXAMPLES

3.1. First example

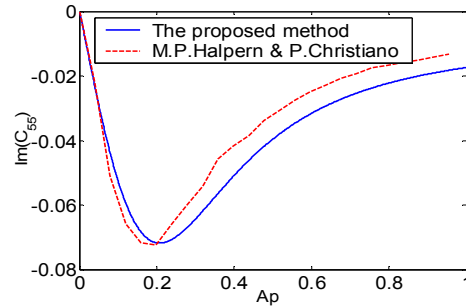
The dynamic vertical and rocking dimensionless compliance for a rigid square plate as a function of the dimensionless frequency are shown in Fig.3.1. The material properties of water-saturated sand, the same as those by M.R.Halpern(1986) for comparison, are summarized in Table 3.1. The results obtained by the method proposed in this paper are compared with those obtained by M.R.Halpern(1986) . The trends are the same for the results obtained by these two methods.

Table 3.1. Material properties for a water saturated coarse sand

ν	0.3	n	0.48
ρ_s	2673 kg / m^3	k	$2.607 \times 10^{-7} \text{ sm}^3 / \text{kg}$
ρ_w	994 kg / m^3	E_s	$2.742 \times 10^8 \text{ pa}$
ζ	0.02	G_s	$9.78 \times 10^7 \text{ pa}$



(a) Real part of C_{55}



(b) Imaginary part of C_{55}

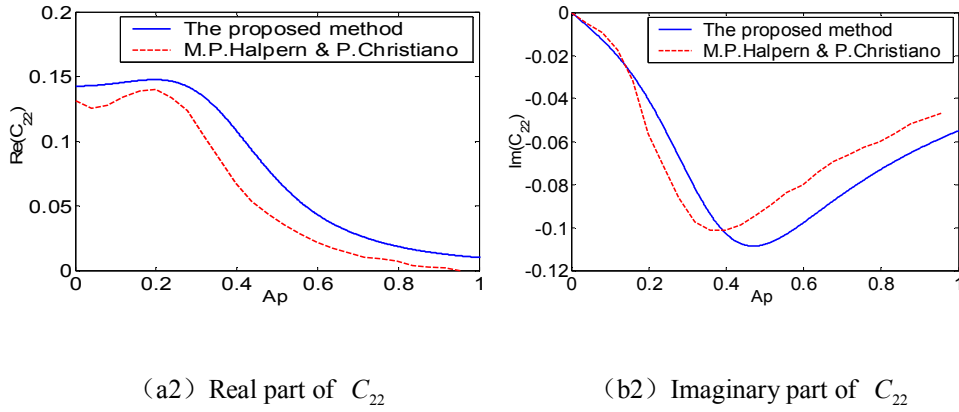
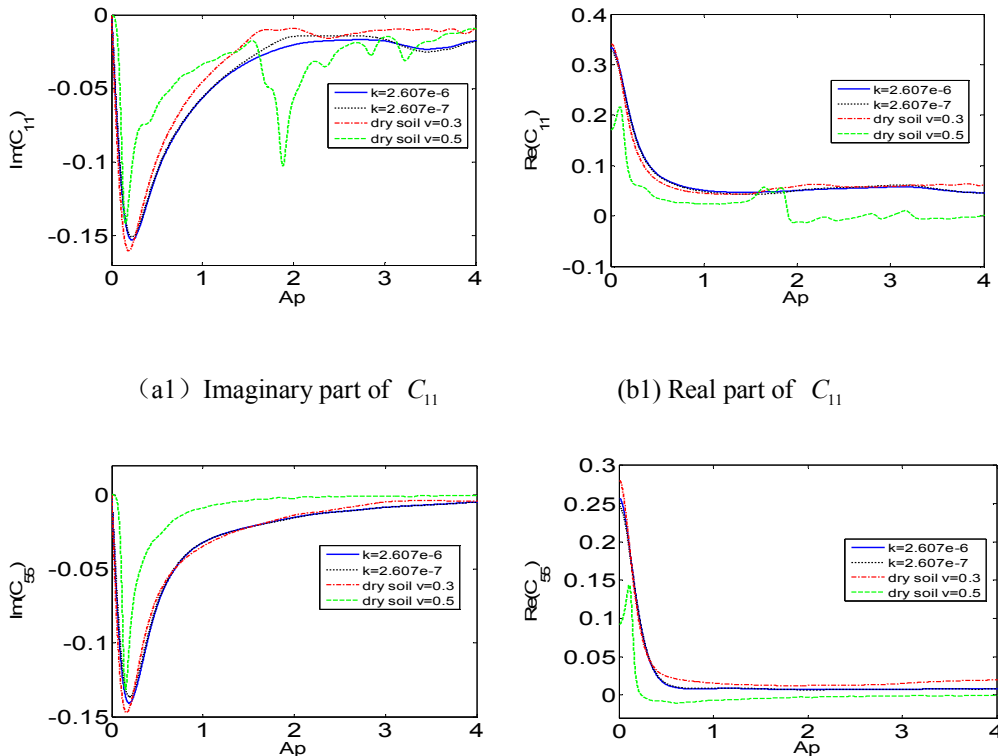


Figure 3.1 Dimensionless vertical compliance function C_{55} and rocking compliance function C_{22} for a rigid square plate

3.2. Second example

3.2.1 Effect of permeability

To check the effect of permeability on dynamic compliance, the results for porous soils with $k = 2.607 \times 10^{-6} \text{sm}^3 / \text{kg}$ and $k = 2.607 \times 10^{-7} \text{sm}^3 / \text{kg}$ are compared with those for drained (corresponding dry soil for the same Poisson ratio) and undrained soil (corresponding dry soil for the Poisson ratio $\nu = 0.5$) in Fig.3.2. At very low dimensionless frequency A_p the poroelastic solutions agree closely with the results for a rigid plate overlying a completely drained soil. This close comparison of results indicates that either the plate is sufficiently small or the period of excitation is sufficiently long to allow nearly complete drainage beneath the plate over the course of each cycle of harmonic excitation. The real part of compliance increases with permeability. The absolute value of imaginary part also increases with permeability.



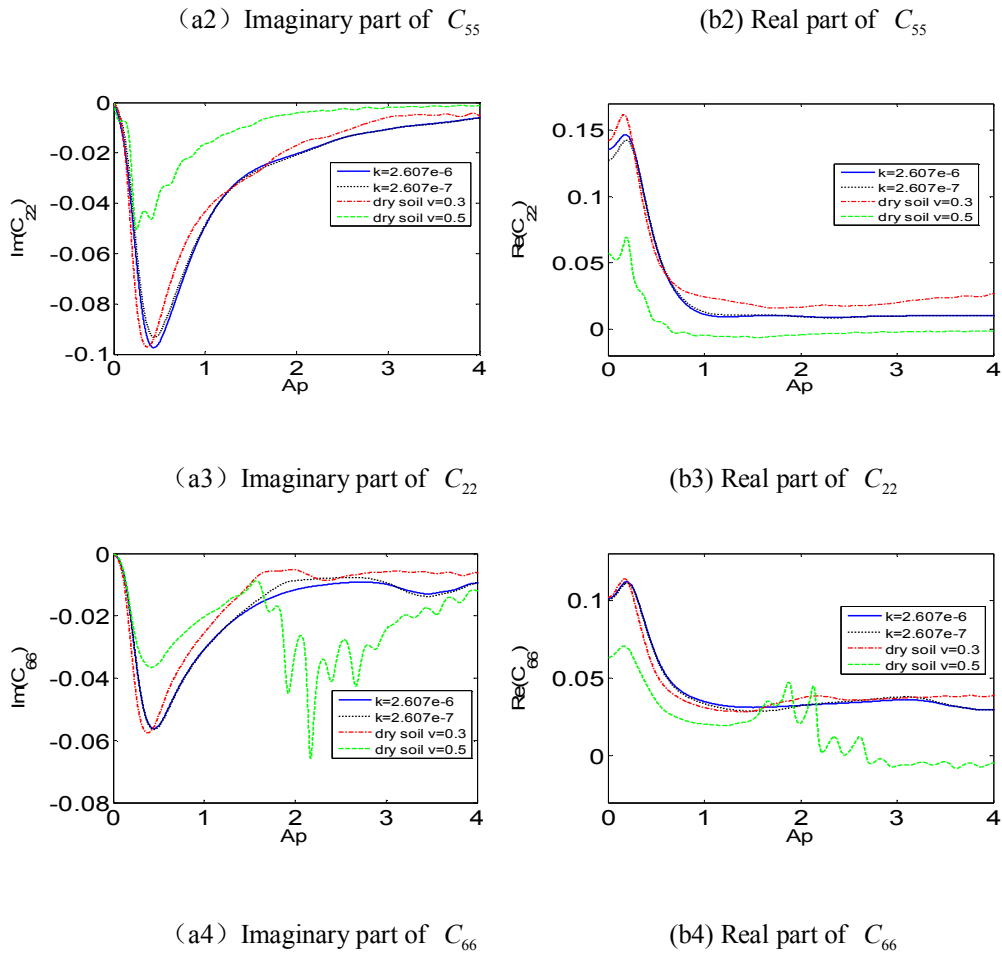
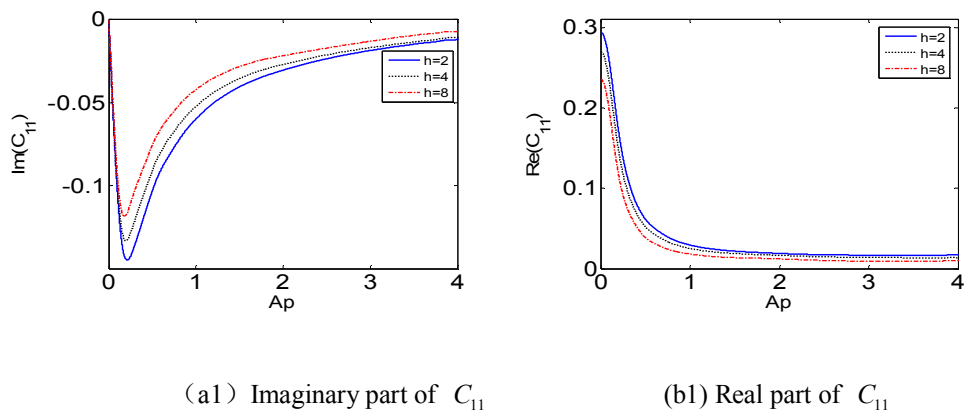
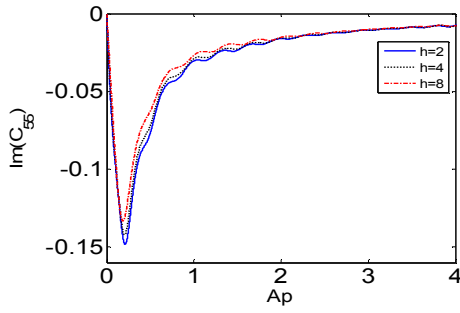


Figure 3.2 Dimensionless compliance function for different permeability

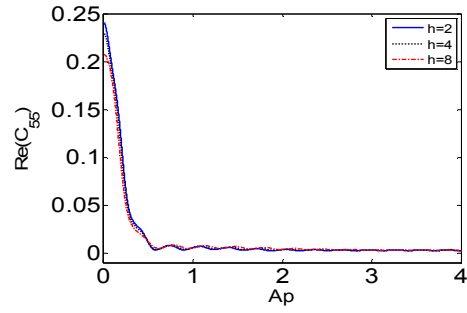
3.2.2 Effect of embedded depth

The properties of the poroelastic half-space are the same as in the first example. The results with embedded depth $D = 2m, 4m, 8m$ are shown in Fig.3.3. The real part of compliance decreases with depth, and the absolute value of imaginary part also decreases with depth. The effect of depth on the vertical compliance is small.

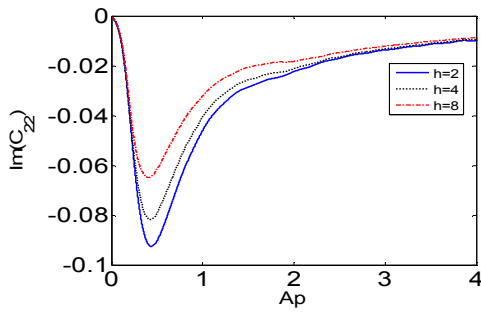




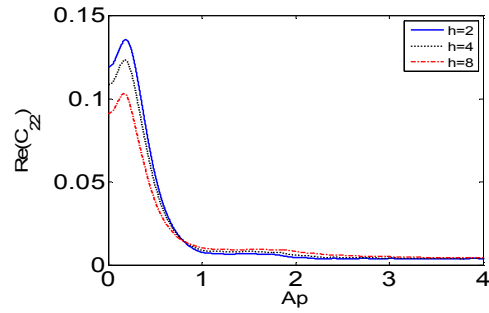
(a2) Imaginary part of C_{55}



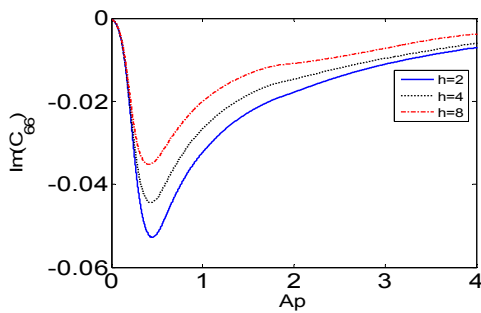
(b2) Real part of C_{55}



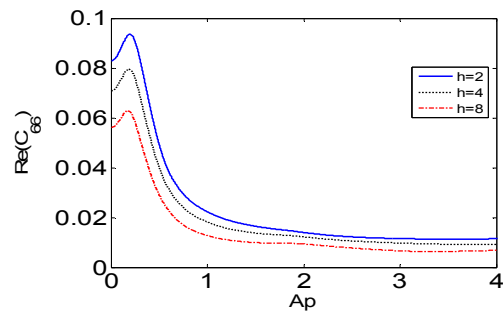
(a3) Imaginary part of C_{22}



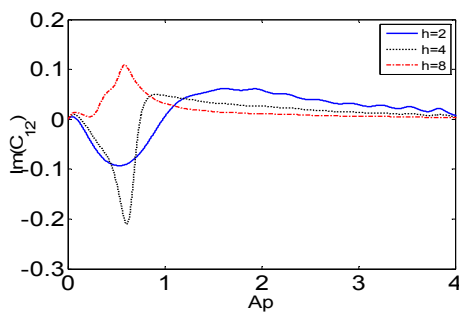
(b3) Real part of C_{22}



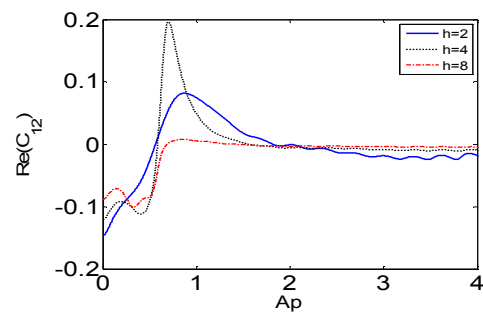
(a4) Imaginary part of C_{66}



(b4) Real part of C_{66}



(a5) Imaginary part of C_{12}



(b5) Real part of C_{12}

Figure 3.3 Dimensionless compliance function for different embedded depth

4. CONCLUSIONS

An FEM method combined with local transmitting boundary for computation of dynamic compliance of foundations resting on porous saturated soils has been presented in this paper. The approach has been applied to the calculation of the dynamic compliances of rectangular plate on a fluid-filled poroelastic half-space. The results obtained are in agreement with the results obtained by Halpern(1986). The effects of the permeability and the embedded depth on the computed compliance functions have been analyzed. The following conclusions can be drawn from the results for plate foundation and the range of dimensionless frequency 0-4:

- (1)The real part of compliance increases with permeability. The absolute value of imaginary part also increases with permeability.
- (2)The real part of compliance decreases with depth, and the absolute value of imaginary part also decrease with depth. The effect of depth on the vertical compliance is small.

The study of more complicated geometries of the soil zones and irregular foundations can be conducted without difficulty.

AKNOWLEDGEMENT

The authors gratefully acknowledge the financial support of this work by the National Natural Science Foundation of China (No.50978135, No.51178222)

REFERENCES

- Biot, M.A. (1956). Theory of propagation of elastic waves in a fluid-saturated porous solid, I: low frequency range. *J. Acoust. Soc. Am* **28**:168-178.
- Halpern, M.R. and Christiano, P. (1986). Steady-state harmonic response of a rigid plate bearing on a liquid-saturated poroelastic half space. *Earthquake Engineering and Structure Dynamics* **14**:439-454.
- Kassir, M.K. and Xu, J.M. (1988). Interaction functions of a rigid strip bonded to saturated elastic half-space. *Int. J. Solids. Struct.* **24**:9,915-936.
- Bougacha, S., Roesset, J.M. and Tassoulas, J.L. (1993). Analysis of foundations on fluid filled poroelastic stratum. *J. Eng. Mech. ASCE* **119**:8,1632-1648.
- Bougacha, S., Roesset, J.M. and Tassoulas, J.L. (1993). Dynamic stiffness of foundations on fluid filled poroelastic stratum. *J. Eng. Mech. ASCE* **119**:8,1649-1662.
- Chen, J. and Dargush, G.F. (1995). Boundary element method for dynamic poroelastic and thermoelastic analysis. *Int. J. Solids. Struct.* **32**:15,2257-2278.
- Chopra, M.B. and Dargush, G.F. (1995). Dynamic analysis of axi-symmetric foundations on a poroelastic stratum using BEM. *10th Engrg. Mech. Spec. Conf., ASCE*. **2**:1046-1049.
- Japon, B.R., Gallego, R. and Dominguez J. (1997). Dynamic stiffness of foundations on saturated poroelastic soils. *J. Eng. Mech. ASCE*. **123**:11,1121-1129.
- Philippacopoulos, A.J. Axisymmetric vibration of disk resting on saturated layered half space. *J. Eng. Mech. ASCE*. **115**:10,2301-2322.
- Rajapakse, R.K.N.D. and Senjuntichai, T. (1995). Dynamic response of a multi-layered poroelastic medium. *Earthquake Eng. Struct. Dyn.* **24**,703-722.
- Chen, S.L., Liao, Z.P. and Chen, J. (2007). A decoupling FEM for simulating near-field wave motions in saturated porous media. *International Journal of Structural Engineering and Mechanics*. **25**:3,181-200.
- Liao, Z.P. and Wong, H.L. (1984). A transmitting boundary for the numerical simulation of elastic wave propagation. *Soil Dyn. Earthq. Eng.* **3**:1,174-183.
- Chen, S.L. and Liao, Z.P. (2003). Multi-transmitting formula for attenuating waves. *Acta Seismological Sinica*. **16**:3,283-291.